

# GEOPHYSICAL INVESTIGATION OF SUSPECTED SPRINGS IN AJEGUNLE-IGOBA, NEAR AKURE, SOUTH WESTERN NIGERIA

M. O. OLORUNFEMI, J. S. OJO, A. I. OLAYINKA, and M. Z. MOHAMMED

(Received 4 September 1999; Revision accepted 24 August 2000)

## ABSTRACT

A geophysical survey, comprising spontaneous potential (SP) and electrical resistivity methods, has been conducted at suspected spring sites in Ajegunle-Igoba, north of Akure, southwestern Nigeria, in order to understand their nature and groundwater development feasibility. The SP survey utilised the fixed array technique along 4 traverses while the resistivity measurement involved 13 Wenner vertical electrical soundings (VES) and 7 dipole-dipole profiles.

The SP profiles display short wavelength negative amplitude anomalies, one of which coincides with a groundwater seepage zone. Three major subsurface layers were identified from the VES interpretation, and these include the topsoil, weathered zone and fresh basement, with the weathered zone constituting the main aquifer. Their resistivities are between 14 to 121  $\Omega\text{m}$ , 145 to 364  $\Omega\text{m}$  and 1750  $\Omega\text{m}$  to infinity, respectively. The overburden is generally thin at less than 20 m thick. The basement rock gave no indication of intense fracturing.

The inverted dipole-dipole pseudosections delineate distinct low resistivity closures within the overburden, which in some cases extend to the basement. The centres of some of these closures are located beneath the seepage zones. Some of the centres correlate to evolve a feature suspected to be a major geological interface through which the groundwater seeps.

Groundwater development in the study area is not feasible due to the thin overburden, low fracture density and the seasonal nature of the seepages.

**KEY WORDS** : spring, spontaneous potential, vertical electrical sounding, dipole-dipole pseudosection, resistivity inversion, Nigeria.

## INTRODUCTION

Structural features with hydrogeological significance in crystalline basement complex rocks include faults, lithological contacts/boundaries, dykes, network of joints, fractures/fissures and shear zones. These geological features may deform the basement rocks creating inhomogeneities which in turn enhance groundwater storage, aid groundwater flow, and the occasional appearance of seepages or springs.

There are different types of springs. Some are related to the arrangement of pervious and impervious layers (e.g stratum springs, overflow springs, valley springs and bourne springs) while others are controlled by geological structures (e.g. joint springs and fault springs). Spring is an excellent source of potable water which rarely requires treatment. When the storage capacity is large, it can

sustain a large community. Ajegunle-Igoba is a small farm settlement, with a population of about 1000 inhabitants and situated about 10 km north of Akure in southwestern Nigeria (Fig. 1). It experiences groundwater seepages during the peak of the rainy season, between June and October (Akintola, 1986). An appreciable volume of water is continuously discharged from the two major locations marked A and B in Fig. 2 and this leads to flooding of the adjoining motorway.

The area is underlain by Precambrian Crystalline Basement Complex rocks that are susceptible to faulting and fracturing. It was thought that if these geological features extend to the surface they might serve as conduits for groundwater and discharge points for seepages and springs. The settlement is bordered in the east by a porphyritic granite ridge which slopes steeply towards the settlement with an attendant high surface runoff. It is probable that part of the runoff

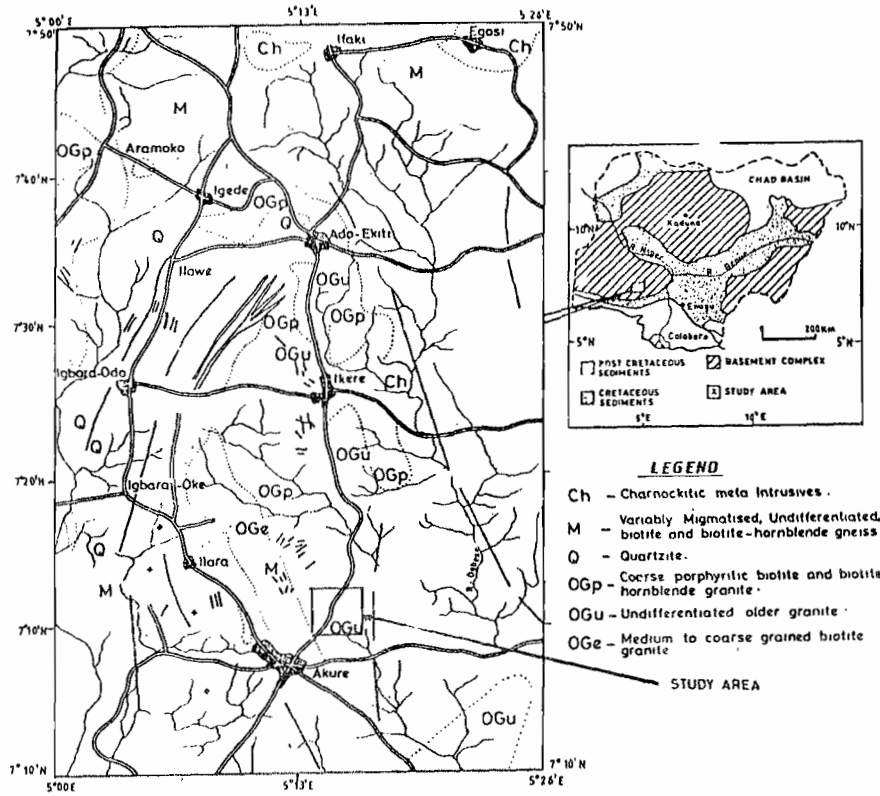


Fig. 1. Regional geologic map of the Akure-Ada-Ekiti area

water could seep underground at the interface between the granite exposure and the topsoil at the base of the ridge and later finds its way out as seepages through zones of discontinuities, such as faults. It was the need to understand the nature of the groundwater seepages at Ajegunle-Igoba and to evaluate its

potential for development into a water supply project that necessitated the present geophysical investigation. The choice of suitable geophysical methods was informed by the fact that water-bearing faults, fractures and fissure zones in the Nigerian basement terrains display relatively low resistivity anomalies (Olorunfemi et al., 1986) while streaming potentials (a component of SP) are produced by groundwater flow through geological conduits (faults, joints, fractures, etc) (Bogoslovsky and Ogilvy, 1970; Black and Corwin, 1984; Butler and Llopis, 1990). The study, therefore, involved the spontaneous potential (SP) and electrical resistivity methods.

## Site description, Geology and Hydrogeology

Ajegunle-Igoba is located along the Akure-Ado Ekiti road (Fig 1). It lies between latitudes 7° 17'N and 7°19'N and longitudes 5°13' E and 5°15'E. The settlement is located in a

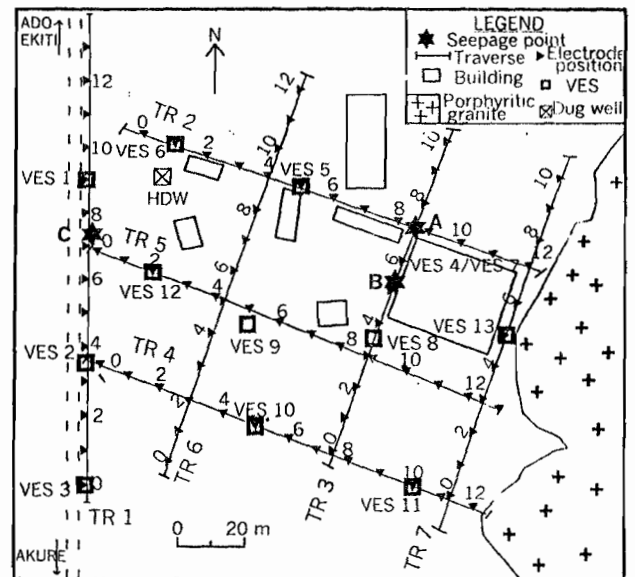


Fig. 2. Enlarged map of the Ajegunle-Igoba area showing the geophysical traverses used in the present study.

relatively flat terrain which gently slopes westward. It is, however, bordered in the east by a porphyritic granite ridge (Fig. 2) which slopes steeply towards the settlement with a tendency for high surface water runoff. The topographical elevation ranges from 354 m to 365 m asl.

The dominant rock type in the study area is porphyritic granite (Dempster, 1966;

Olawejaju, 1981), and it occurs as ridges/hills and low-lying units. The rock is greyish in colour, being rich in leucocratic minerals notably feldspars (microcline and microperthites) and quartz. The other minerals present are biotite and hornblende. The strike of foliation is approximately N-S. The texture is coarse grained.

Crystalline basement complex rocks are characterised by low primary porosity and negligible permeability. Groundwater is known to accumulate within the weathered and/or fractured basement zones (Olayinka and Olorunfemi, 1992; Olorunfemi and Fasuyi, 1993). The nature and extent of weathering vary considerably, depending upon the presence of fractures at depth and favourable morphological features at the surface (Satpathy and Kanungo, 1976; Verma et al., 1980).

The effective porosity and permeability of basement aquifers vary widely resulting in a large range of yields. The water storage capacity mainly depends upon the total thickness of the weathered and fractured zones. The groundwater level observed from a hand-dug well (denoted as HDW in Fig. 2) at the time of the present investigation in September 1995 was shallow at 1.5 m below the ground level.

**METHOD OF STUDY**

Seven geophysical traverses were established in the study area (Fig. 2), along the following azimuths : 0° (TR 1), 20° (TR 3, 6

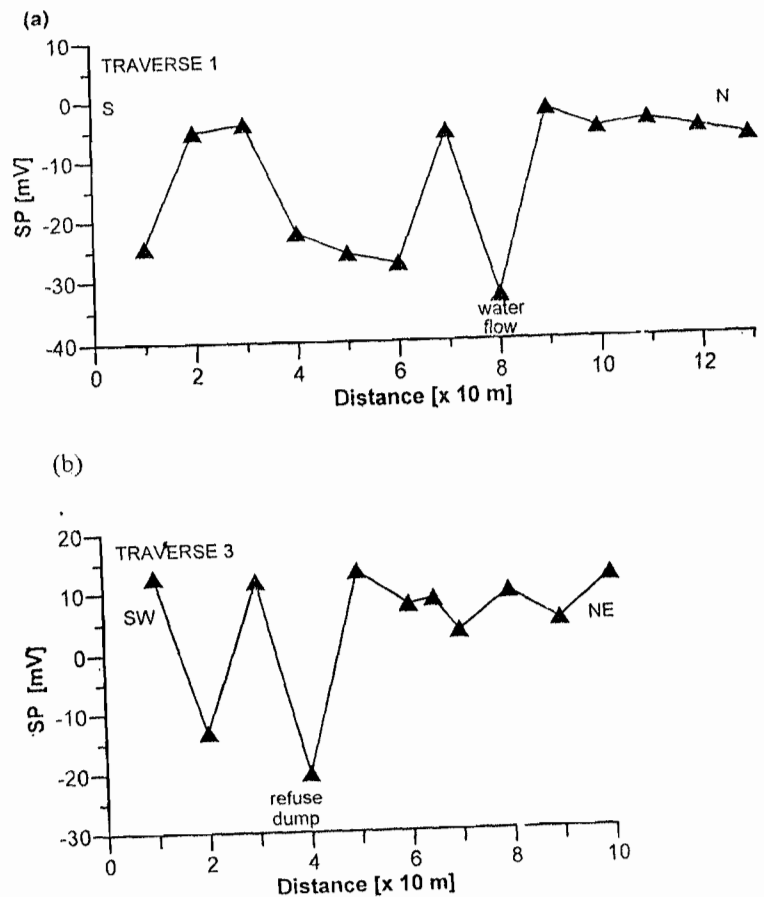


Fig 3. SP profiles measured along two S-N lines. The position marked "water flow" was observed in the field.

and 7) and 110° (TR 2, 4 and 5). The traverses range in length from 100 to 140 m, and were marked out at 10 m station intervals. Spontaneous potential (SP) and electrical

Table 1. Geoelectric parameters obtained from VES modelling and inversion

Geoelectric/ Geologic layer	Description	Geoelectric parameters	
		Resistivity (Ωm)	Thickness (m)
topsoil	clay/sandy clay and clayey sand	14 to 121	0.4 to 2.1
weathered zone	sandy clay/clayey sand	145 to 364	1 to 17
*partly weathered / fractured	basement	568	7
fresh basement	basement	1750 to ∞	

\*very localised; identified beneath VES 3 only.

NB. The depth to rock head ranges between 2 and 20 m.

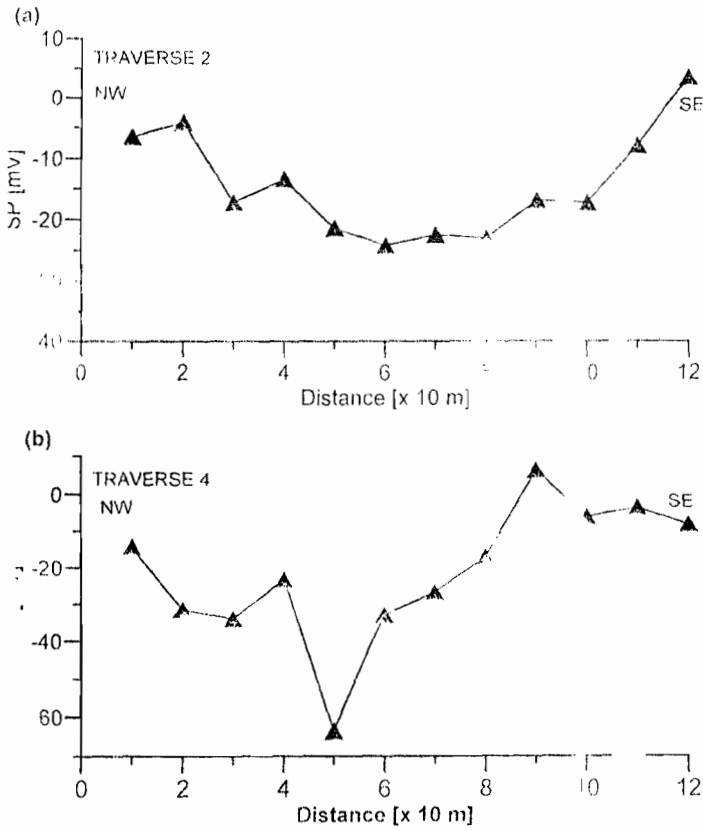


Fig 4. SP profiles measured along two NW-SE lines.

resistivity measurements were made. Total field SP data were acquired along Traverses 1 to 4 while dipole-dipole resistivity profiling data were measured along all the seven traverses.

The inter-electrode spacing employed was 10 m and the expansion factor,  $n$ , was varied from 1 to 5. Thirteen vertical electrical soundings (VES) were also carried out, using the Wenner array, with a maximum electrode spacing of 64 m.

The SP data are presented as profiles while the resistivity data are plotted as depth sounding curves, pseudosections and map. Interpretation of the SP profiles, resistivity pseudosections and map involved the detection of signatures or patterns that are diagnostic of fluid flow and fluid flow paths such as lithological contacts, faults and fracture zones and similar zones of discontinuity.

Quantitative interpretation of the depth sounding curves involved partial curve matching and computer assisted inversion. Geoelectric sections have been prepared from the 1-D sounding interpretation, and these were used as the starting models for a 2-D inversion algorithm based on the Simultaneous

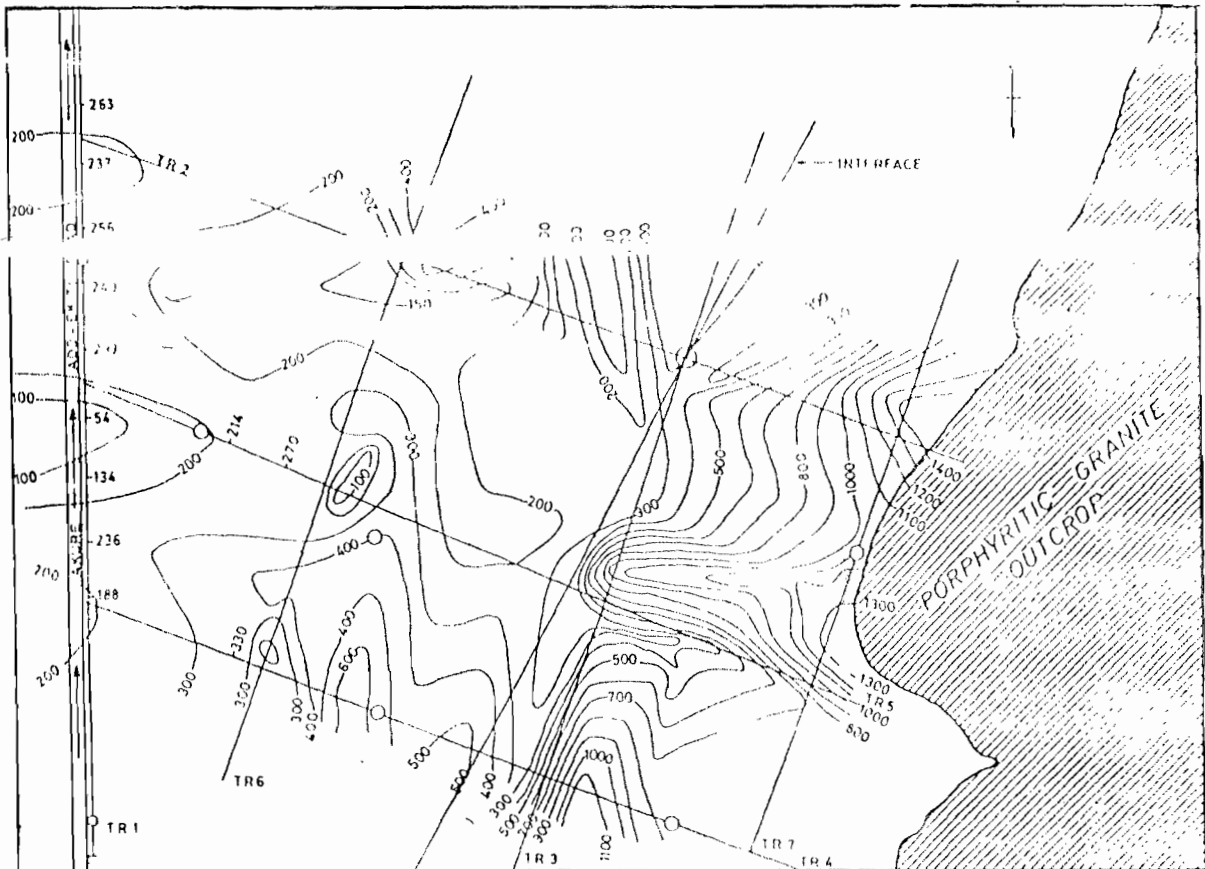


Fig 5 Dipole-dipole resistivity map for  $n = 3$

Iterative Reconstruction Technique (SIRT) (Weller et al., 1996; Olayinka and Weller, 1997) for interpretation of the pseudosection data.

The 2-D program uses a finite difference approach (Dey and Morrison, 1979) to solve for the potential distribution due to point sources of current. The modelling routine accounts for 3-D sources (current electrodes) in a 2-D material model. This implies that the resistivity can vary arbitrarily along the line of surveying (x-direction) and with depth (z-direction), but the models have an infinite extension along the strike or y-direction. The forward problem for each current source is solved separately and the apparent resistivities for any desired configuration are computed by a superposition of several pole-pole configurations. In the case of multi-electrode arrays this procedure reduces the number of forward problems to the number of current electrodes, which is generally much lower than the number of measured configurations.

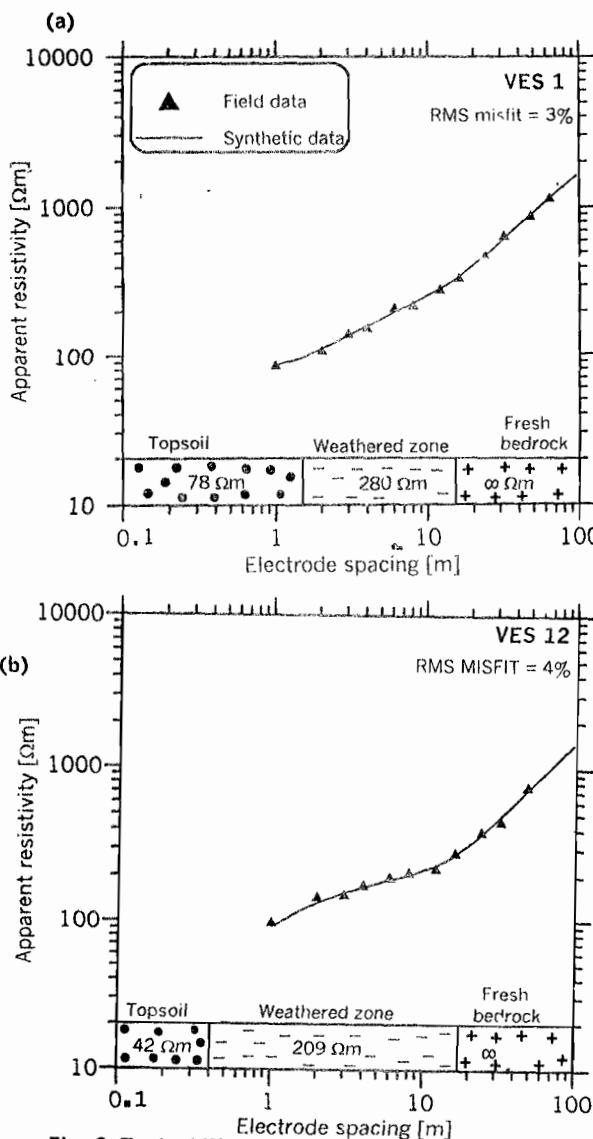


Fig. 6. Typical Wenner sounding curves from the study area and their interpretation.

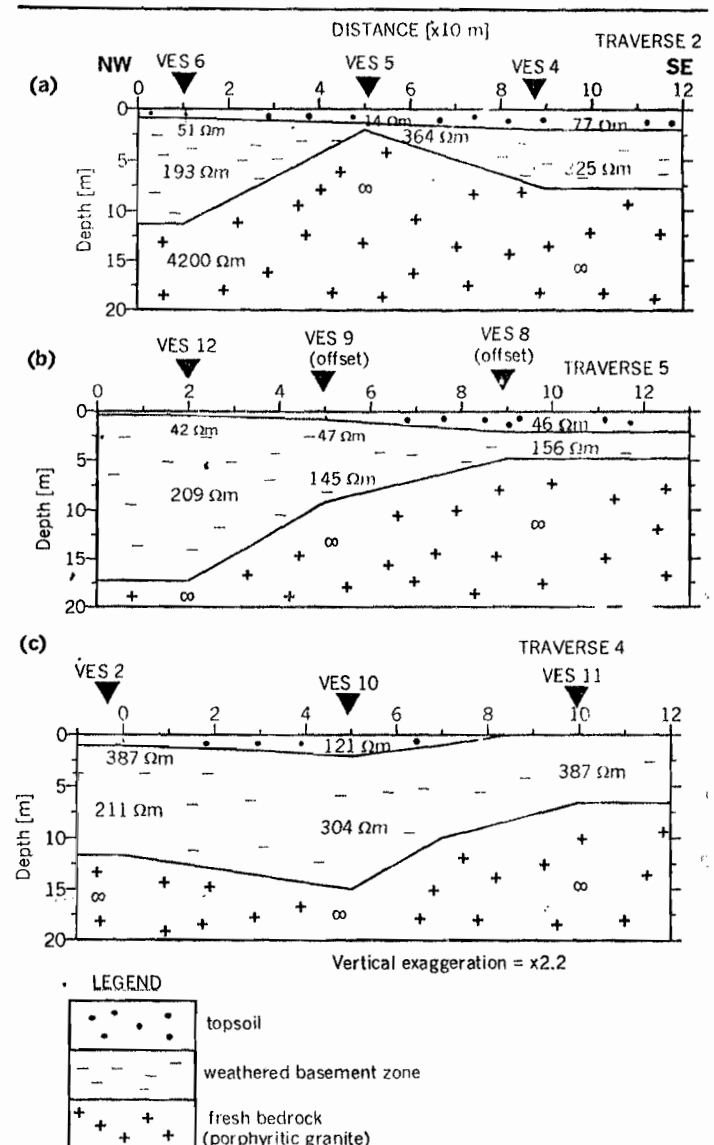
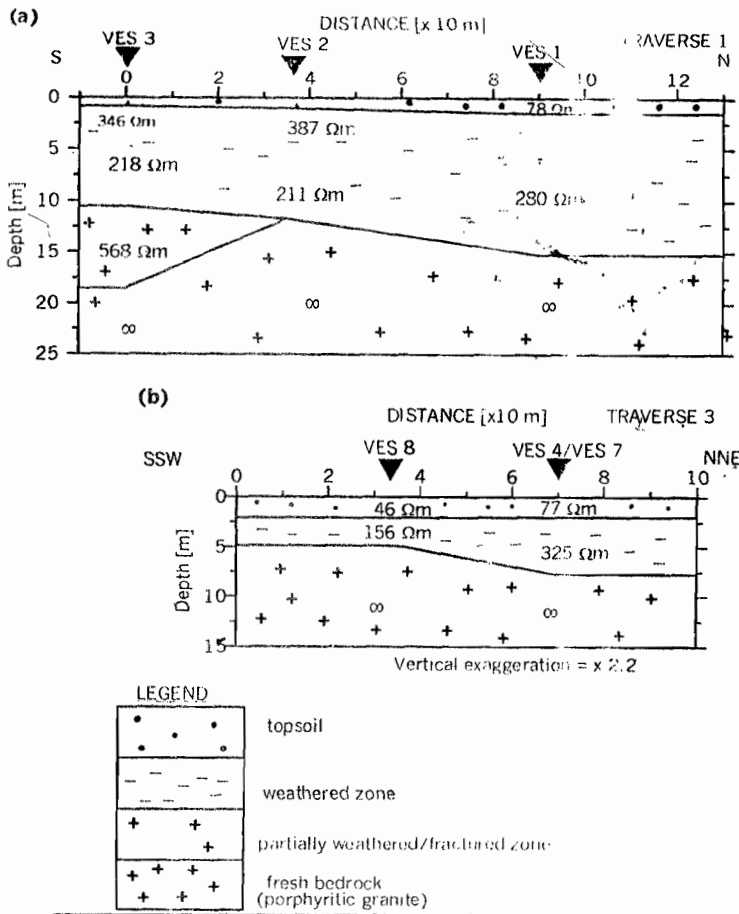


Fig 7. Goelectric section along the NW - SE traverses, as interpreted from VES data.

A rectangular grid was used, which coarsens away from the centre of the air-earth interface. Each node on the grid is assigned a particular resistivity. Discretization errors, which are caused by the inadequate approximation of the introduction of current at a point by the finite difference grid, are removed considerably by the application of a singularity removal (Lowry et al, 1989). To further improve the accuracy, the minimal and maximal discrete wavenumbers are chosen according to the the maximal and minimal distances, respectively, between the current and potential electrodes. The precision of the inverse Fourier transform can also be improved by increasing the number of discreté wavenumbers per decade. Six wavenumbers per decade are used in the present work and gave a sufficient precision.



features such as fractures, fissures or lithological contacts with potential for seepage. It has been shown (Butler et al., 1989) that an idealised seepage-induced total field SP anomaly is a single SP low, with the position of the peak negative amplitude located directly above the seepage zone.

### Dipole-dipole resistivity map

Figure 5 presents a dipole-dipole apparent resistivity map for the expansion factor  $n=3$ , with a theoretical depth of investigation of about 10 m (Roy and Apparao, 1971). This map shows a transition from high apparent resistivity (greater than about 500 Ωm) near-surface basement zone in the east (in vicinity of the porphyritic granite outcrop) to low apparent resistivity (less than about 300 Ωm) in the west where the overburden is expected to be relatively thicker.

### Sounding curve interpretation

The VES curves comprise two-layer type, three-layer A-type, four-layer KH-type to five-layer KHA-types (Fig 6), with the A-type predominating. Two geoelectric sections are presented in Figs 7 and 8. As is common with

Fig 8. Geoelectric section for traverses 1 and 3, as interpreted from VES data.

## RESULTS AND DISCUSSION

### SP profiles

The observed SP values (Figs 3 and 4) generally vary from about +13 to -64 millivolts. Traverse 1 (Fig 3a) shows two anomalies with peak negative amplitudes between stations 4 and 6 and at station 8 respectively. The anomaly at station 8 coincides with a minor water seepage zone C (Fig. 2). The SP profile along traverse 3 (Fig 3b) shows two SP anomalies with peak negative amplitudes at stations 2 and 4, respectively. The latter is located on a refuse dump which may have influenced the SP response.

The SP profile measured along Traverse 2 (Fig. 4a) displays a broad anomaly with peak negative amplitudes between stations 4 and 9. The SP profile along Traverse 4 (Fig 4b) displays a single anomaly with peak negative amplitude located midway between stations 4 and 5.

Although only one of the short wavelength SP anomalies coincides with a groundwater seepage zone, it is suspected that some others (e.g. one along TR4) may be diagnostic of concealed water-bearing, narrow, near-surface

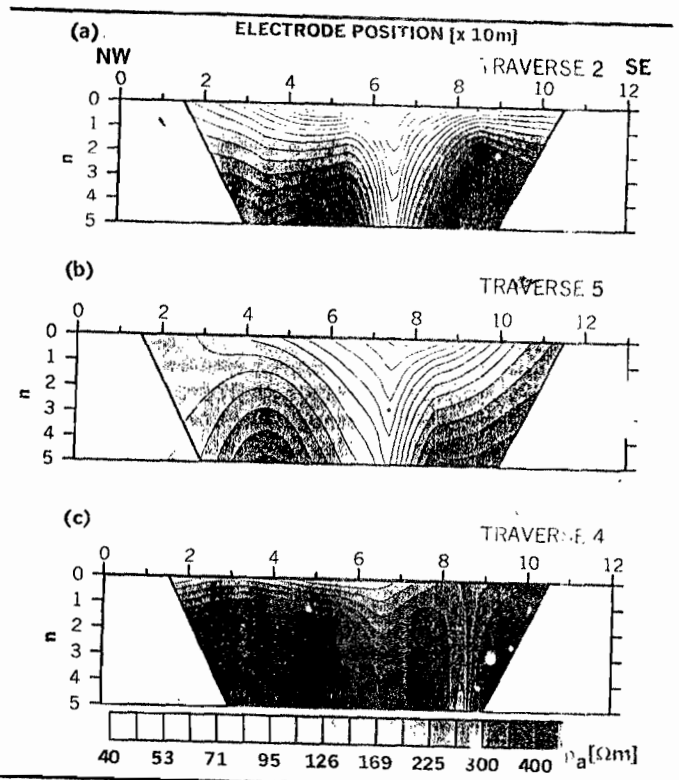


Fig 9. Measured apparent resistivity pseudosection data along NW-SE traverses in the study area.

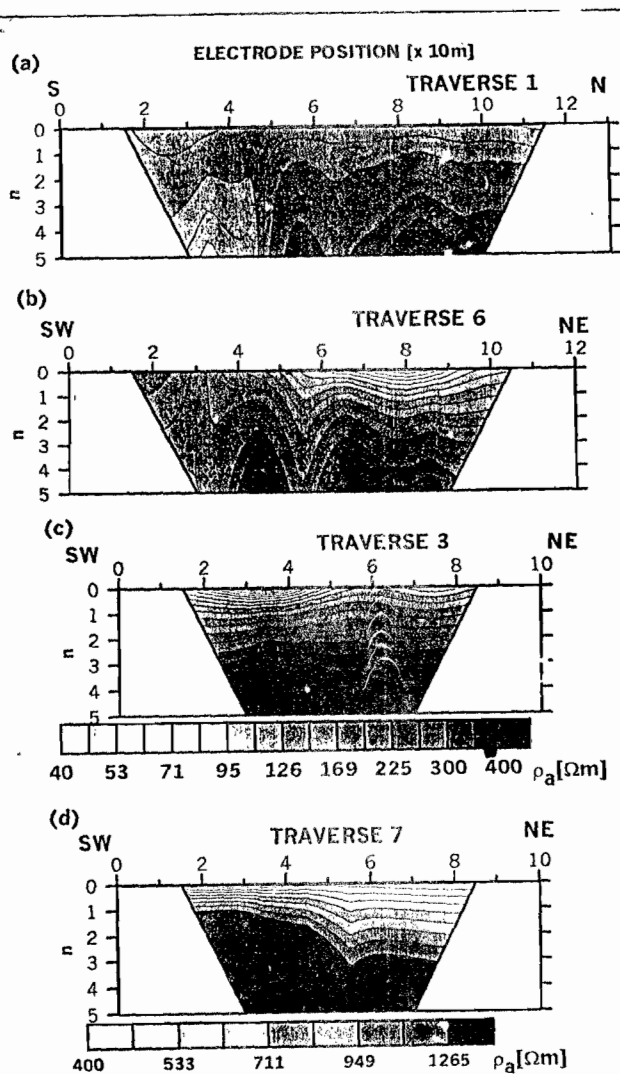


Fig 10. Measured apparent resistivity pseudosection data along the S-N traverses.

Precambrian basement areas within low latitudes (Olorunfemi et al., 1986), four subsurface layers are delineated, namely the topsoil, weathered zone, partly weathered/fractured basement and fresh basement. However, the general tendency in appreciable development of a thick low resistivity the study area is for the resistivity to increase with depth, without any appreciable development of a thick low resistivity zone within the regolith. The geoelectrical characteristics are summarized in Table 1.

Except beneath VES 3, the geoelectric sections show no indication of any significant basement fractures. The overburden is generally shallow at less than 20 m thick. The basement interface dips westward (Figs. 7 and 8), away from the outcropping granite. The storage capacity of the basement aquifer (weathered zone) is low.

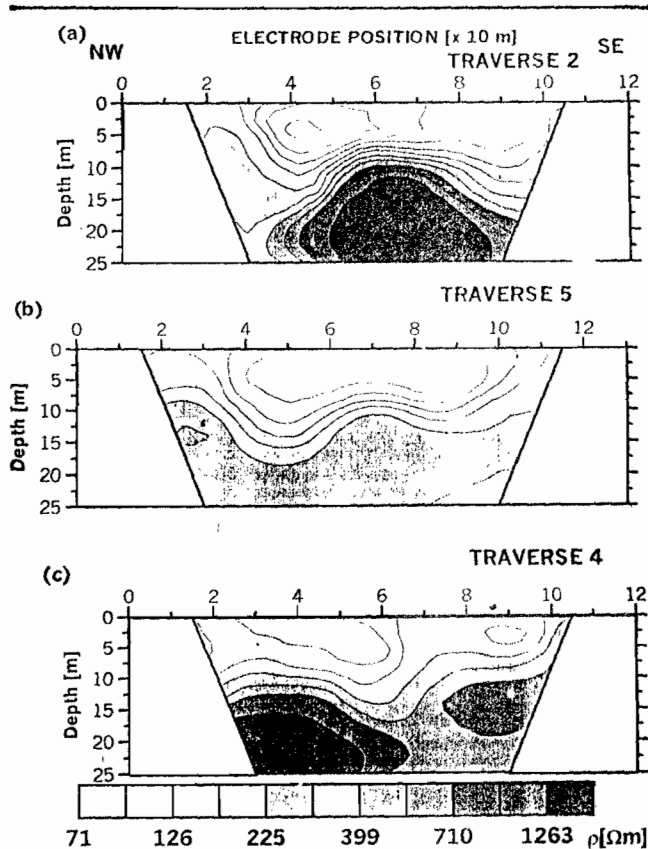


Fig 11. Models from the 2-D inversion of the data in Fig 9.

### Dipole-dipole pseudosections

The measured apparent resistivity dipole-dipole data are shown in Figs 9 and 10. They range from about 26 to 1400 Ωm. The pseudosections are characterized by generally thin near homogeneous overburden with a relatively low resistivity at less than 100 Ωm. This is corroborated by the geoelectric

Table 2. Characteristics of the low resistivity closures identified from 2-D inversion of the pseudosection data

Traverse	Closure characteristics		Identified surface feature
	Region(s)	Centre(s)	
1.	60-80 m	70 m	water seepage at 65 m
2.	30-100 m	45 m	water seepage at 85 m
3.	50-80 m	70 m	water seepage at 70 m
4.	30-60 and 80-100 m	55 and 90 m	none
5.	35 - 60 and 70 - 100 m	45 and 85 m	none
6.	20- 35 m and, 50 - 90 m	30 and 80 m	none
7.	*35 - 65 m	55 m	none

\*Not clearly identified.

NB. The 0 m reference is station 0 along each Traverse.

sections. There are low resistivity anomalies at about electrode positions 6.5 and 7.5 along Traverses 2 and 5, respectively, and between electrodes 6 and 9 along Traverse 4. The basement interface is irregular, judging from the wavy nature of the high resistivity contours at depth.

The observed data, being influenced by the electrode array, may not reflect the true resistivity distribution in the subsurface.

Consequently, inversion of the data was carried out, with the range of equivalence reduced by the imposition of constraints in the form of available geological/geophysical data (Olayinka and Weller, 1997). Using the geoelectric sections as starting models, the field data were interpreted employing the SIRT algorithm. The inverted models after 10 iterations are shown in Figs 11 and 12. Apart

from the fact that the features in the observed pseudosections are significantly preserved in the inverted sections, distinct low resistivity closures, with resistivities of less than 300  $\Omega\text{m}$ , were delineated within the overburden. Some of these closures have appreciable depth extents of over 10 m, especially along Traverses 2, 5 and 6. The regions and centres of the resistivity closures are shown in Table 2.

Low resistivity closures observed along TR 4 to 7 may be concealed potential seepage zones or pockets of low resistivity weathered layer. The apparent resistivities calculated from

the inverted 2-D models are shown in Figs 13 and 14. The misfit between the observed and the calculated data is in the range of 20 to 39%. Most of the features recognisable in the measured data are modelled accurately.

### Integrated interpretation

The zone of an abrupt change in the contour gradient in the apparent resistivity map of Fig 5 corresponds with a geological feature F, shown in Fig 15. Moreover, it is interesting to note that the centres of some of

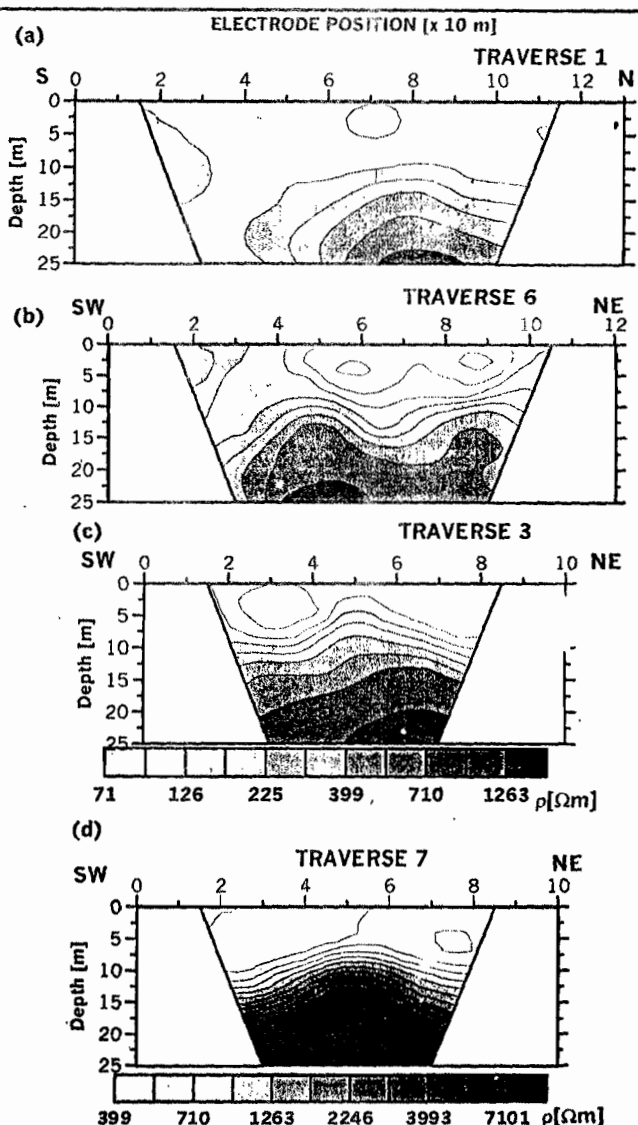


Fig 12. Inverted 2-D models for the respective S-N traverses.

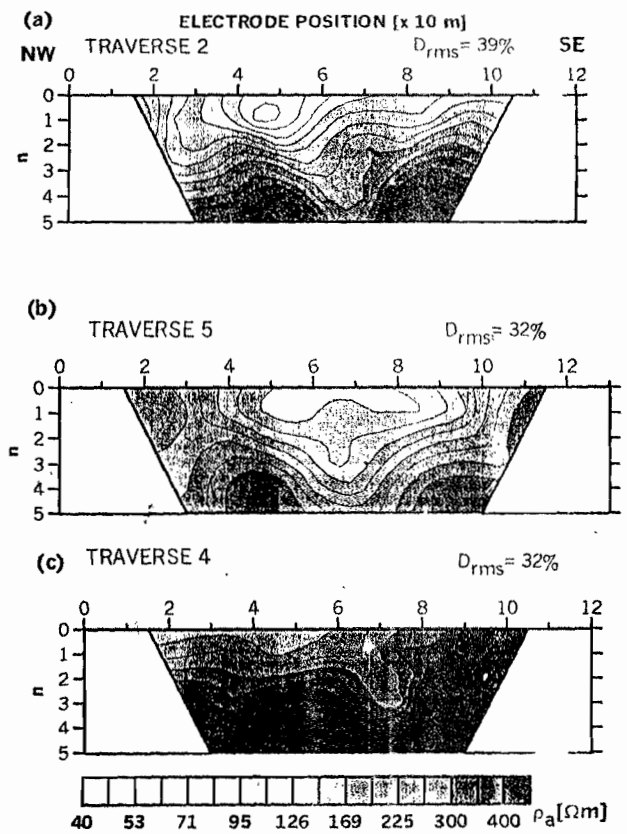


Fig 13. Apparent resistivity pseudosection data calculated from the models in Fig 11.



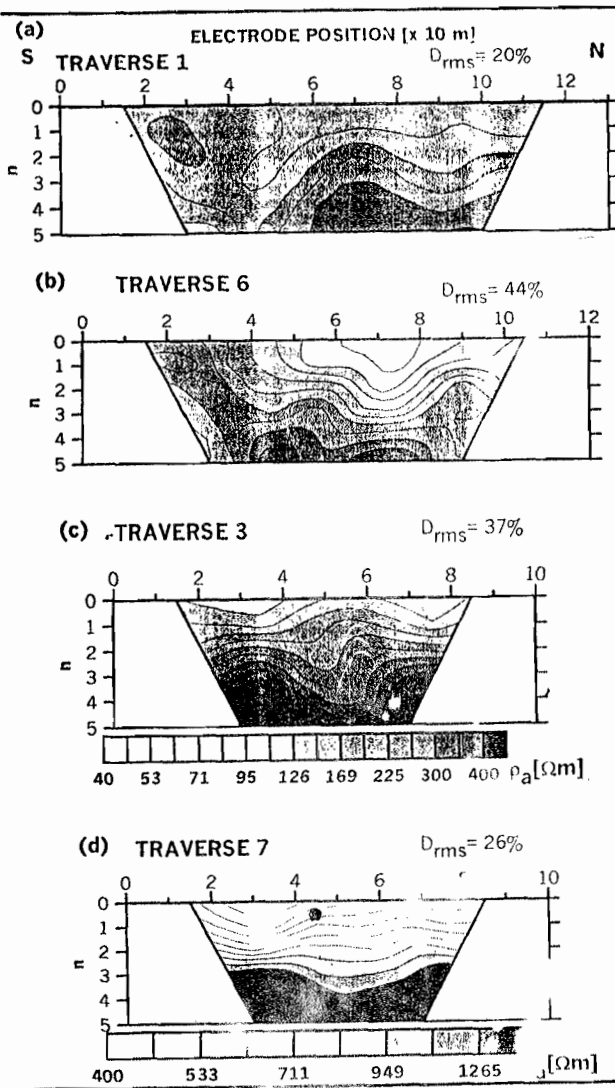


Fig 14. Apparent resistivity pseudosection data calculated from the mode Fig 13.

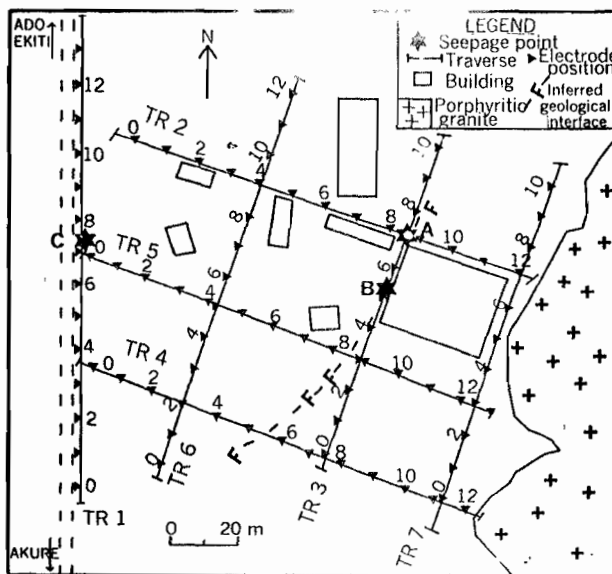


Fig 15. Inferred geological interface through which the groundwater seeps.

the identified closures coincide with seepage points (e.g. along Traverses 1 and 3). Some of these centres correlate across Traverses 2, 5, 4 and 3 to give feature F, suspected to be a geological interface. The groundwater is suspected to seep through this interface.

The basement rock is relatively shallow, at about 6 m below the ground level, in the vicinity of seepage zones A and B, with a tendency for near-surface groundwater table. Persistent rainfall will cause the water level to rise due to groundwater recharge from surface precipitation and basal flow of runoff from the hills thereby enabling water seepage through any near-surface zones of discontinuity, as delineated above. The groundwater recedes with the cessation of the rains and its level eventually falls with consequent stoppage of groundwater seepage. This explains the seasonal nature of the groundwater seepage.

### CONCLUSIONS

The SP profiles display short wavelength (with a width less than 50 m), negative amplitude anomalies (less than 70 mV) which may be diagnostic of water-saturated, narrow, near-vertical geologic interface along Traverses 1, 3 and 4. One of the SP anomalies along TR 1 coincides with a seepage zone.

Three major subsurface layers were identified from the VES interpretation to include the topsoil, weathered zone and fresh basement with resistivity ranges of 14 to 121  $\Omega\text{m}$ , 145 to 364  $\Omega\text{m}$  and over 1750  $\Omega\text{m}$ , respectively. The thicknesses of the topsoil and weathered basement range between 0.4 and 2.1 m and 1 to 17 m, giving a maximum overburden thickness of about 20 m. Partly weathered/fractured basement is generally lacking.

The inverted 2-D models of the dipole-dipole profiling data are characterised by generally thin, near-homogeneous and relatively low resistivity overburden with an irregular bedrock interface. Low resistivity closures are delineated within the overburden which in some cases extend to the basement rocks. This interface correlates with the zone of an abrupt change in gradient of resistivity contours in the dipole-dipole apparent resistivity data. It is thought that the groundwater seeps through this interface. The seasonal nature of the groundwater seepages and the thin overburden might not make development of the suspected springs for groundwater feasible.

## ACKNOWLEDGEMENT

Reviews by Dr. C. S. Okereke and an anonymous referee of this journal have greatly enhanced the clarity of the paper.

## REFERENCES

- Akintola, J.O., 1986. Rainfall distribution in Nigeria 1892-1983. Impact Publishers, Ibadan. 380 pp.
- Black, W.E. and Corwin, R.F., 1984. Application of self potential measurements to the delineation of groundwater seepage in earth-fill embankment. 54<sup>th</sup> Ann. International Mtg. of Soc. Expl. Geophysics. Abstract. pp. 162-164.
- Bogoslovsky, V.A. and Ogilvy, A.A., 1970. Natural potential anomalies as a quantitative index of the rate of water seepage from reservoirs. *Geophysical Prospecting*, 18: 261-268.
- Butler, D.K. and Llopis, J.L., 1990. Assessment of anomalous seepage conditions. US Army Eng. Waterways Expt. Station, Vicksburg, Mississippi. pp. 153-173.
- Butler, D.K., Llopis, J.L., and Deaver, C.M., 1989. Comprehensive geophysical investigation of an existing dam foundation. (Geotechnical Applications 5). *Geophysics: The Leading Edge of Exploration*, August 1989, pp. 10-18.
- Dempster, A.N., 1966. Geological Map of Akure on 1: 250 000, Sheet 61, Geological Survey of Nigeria.
- Dey, A. and Morrison, H.F., 1979. Resistivity modelling for arbitrarily-shaped two-dimensional structures. *Geophysical Prospecting*, 27: 107-136.
- Lowry, T., Allen, M.B. and Shive, P.N., 1989. Singularity removal : a refinement of resistivity modelling techniques. *Geophysics*, 54: 766-774.
- Olarewaju, V.O., 1981. Geochemistry of charnockitic and granitic rocks of the basement complex around Ado Ekiti - Akure, southwestern -Nigeria. PhD Thesis, University of London, 383 pp.
- Olayinka, A.I. and Olorunfemi, M.O., 1992. Determination of geoelectrical characteristics in Okene area and implication for borehole siting. *Journal of Mining and Geology*, 28: 403-412.
- Olayinka, A.I. and Weller, A., 1997. The inversion of geoelectrical data for hydrogeological applications in crystalline basement areas of Nigeria. *Journal of Applied Geophysics*, 37: 103-115.
- Olorunfemi, M.O. and Fasuyi, S.A., 1993. Aquifer types and the geoelectric /hydrogeologic characteristics of part of the central basement terrain of Nigeria (Niger State). *Journal of African Earth Sciences*, 16 (3): 309-316.
- Olorunfemi, M.O., Olarewaju, V.O. and Avci, M., 1986. Geophysical investigation of a fault zone, case history from Ile-Ife, Nigeria. *Geophysical Prospecting*, 34: 1277 - 1284.
- Roy, A. and Apparao, A., 1971. Depth of investigation in direct current methods. *Geophysics*, 36: 201 - 226.
- Satpathy, B.N. and Kanungo, D.N., 1976. Groundwater exploration in hard rock terrain: a case history. *Geophysical Prospecting*, 24: 725 - 736.
- Verma, R.K., Rao, M.K. and Rao, C.V., 1980. Resistivity investigation for groundwater in metamorphic areas near Dhanbad, India. *Groundwater*, 18(1): 46-55.
- Weller, A., Seichter, M. and Kampe, A., 1996. IP modelling using complex electrical conductivities. *Geophysical Journal International*, 127: 387-398.